Numerical Methods in Civil Engineering, 10-1 (2025) 102-112

Numerical Methods in Civil Engineering

Journal Homepage: https://nmce.kntu.ac.ir/

Investigating Groundwater Level Fluctuations using Group Method of Data Handling and Empirical Bayesian Kriging Models (Case study: Silakhor plain)

Mehdi Komasi*, Hesam Goudarzi**

ARTICLE INFO

RESEARCH PAPER

Article history:
Received:
September 2025
Revised:
October 2025
Accepted:
November 2025

Keywords:
Groundwater level,
EBK,
GMDH,
Temporal-Spatial,
Silakhor plain.

Abstract:

Groundwater level fluctuations and the lack of reliable methods for estimating them are major contributors to land subsidence. Data mining has increasingly applied artificial intelligence (AI) techniques in recent years to predict time series variations, including groundwater level changes. In this study, a temporal–spatial hybrid model was developed by integrating the Group Method of Data Handling (GMDH) with Empirical Bayesian Kriging (EBK) to predict monthly groundwater levels. The GMDH model was employed to extrapolate temporal variations one month ahead, while the EBK model interpolated spatial variations to generate regional groundwater level maps. The Silakhor Plain in Iran was chosen as the subject of the case study. The model was built using monthly data from 11 groundwater stations that were collected between 2003 and 2013. The hybrid model employed groundwater level observations and precipitation records as inputs. Results indicated that the GMDH-EBK model provided reliable and accurate predictions, with strong correlations in both training and testing phases. The model achieved coefficients of determination of 0.95, 0.91, 0.85, and 0.79 for the Hamyaneh, Chaghadon, Sugar Factory, and Valyan wells, respectively. Overall, the proposed methodology represents a significant advancement in regional groundwater modelling and offers a promising approach to supporting sustainable water resource management.

1. Introduction

Recently, artificial intelligence (AI) has demonstrated great effectiveness in modelling and forecasting non-linear hydrological time series. These techniques excel at handling large volumes of dynamic, non-linear, and noisy data, particularly when the underlying physical relationships are not fully understood. This makes AI an ideal tool for data-driven time series modelling, as it doesn't require prior knowledge of the process being simulated. Groundwater level modelling, along with other hydrological processes, is crucial for effective urban and environmental planning, as well as water resource management within a watershed. Such models are also vital for mitigating the effects of drought on water systems.

Over time, numerous hydrological models have been developed to simulate these complex processes, with a detailed classification provided by Nourani et al. [1]. Assessment and prediction concerning groundwater levels through specific models may contribute to groundwater resources predictions [2]. Monitoring groundwater level fluctuations is critical for sustainable water resource management, as it provides essential insights into the balance between recharge and extraction, helping to prevent overexploitation and land subsidence. These fluctuations are key indicators of aquifer health, influencing agricultural productivity, urban planning, and ecosystem stability, particularly in water-scarce regions like Iran. Accurate monitoring enables early detection of drought impacts, informs policy decisions on irrigation and industrial water use, and supports the design of effective mitigation strategies to address declining groundwater reserves,

* *Corresponding author: Associate Professor, Department of Civil Engineering, Ayatollah Boroujerdi University, Boroujerd, Iran. E-mail: Komasi@abru.ac.ir.*
** *M.Sc., Department of Civil Engineering, Ayatollah Boroujerdi University, Boroujerd, Iran. goudarzi.h@email.kntu.ac.ir*

https://doi.org/10.61882/NMCE.2508.1100

thereby ensuring long-term environmental and economic resilience.

The use of data-driven models for time series prediction has been increasing steadily [3-5]. Designing groundwater observation networks is often considered a multi-objective optimization problem. Dealing with spatial and temporal variability demands significant time and computational power [6-8]. To overcome these challenges, researchers have combined geostatistical models, optimization algorithms, and AI methods. Artificial Neural Networks (ANNs), in particular, have been widely adopted because of their computational efficiency and ability to learn nonlinear patterns. Over the past decades, ANNs have been increasingly applied in water resources research, yielding encouraging results [9]. Several recent studies have employed various artificial neural networks (ANNs) to model groundwater time series [10-17].

One type of artificial neural network (ANN) is the Group Method of Data Handling (GMDH). This model has been successfully applied to address uncertainty as well as linear and nonlinear system behaviours across a wide range of disciplines, including engineering, science, economics, signal processing, and control systems [18-19]. The GMDH model employs an inductive learning algorithm to identify relationships between input and output variables, optimizing the network structure through quadratic regression polynomials based on two input variables [20]. A general limitation of ANNs arises in situations where the solution space is short-tailed, where a small number of features dominate the solution. In such cases, continuous features may not rely on a smooth gradient (for example, raw measures such as the duration a user remains on a page after clicking are poor predictors in an ANN). Consequently, insufficient data are often available to train such complex models effectively. To solve problems related to prediction, system identification, and control, the GMDH (which was first introduced by Ivakhnenko in 1968 [21]) provides an objective high-order polynomial representation of input variables. Through a process of self-organization, GMDH iteratively generates, evaluates, and selects candidate networks of increasing complexity, characterized by larger numbers of parameters, parameter interactions, and nonlinear structures, until an “optimal” model is achieved [22]. The adoption of GMDH as an artificial intelligence tool has grown steadily (e.g., [20, 22]), with notable applications in hydrological research [18, 23-25]. However, its application in groundwater studies remains relatively limited. Despite its advantages, GMDH is primarily designed for time series analysis, whereas in certain contexts, spatially explicit models are required to capture and assess spatial variability.

Geostatistical methods are particularly useful for interpolating spatial parameters such as groundwater elevation. These approaches allow the prediction of unknown values by exploiting available spatial information. Consequently, the geostatistical modelling of climatic variables, such as monthly precipitation, has become a key area of interest for climatologists and hydrologists [26-27]. A variety of interpolation techniques have been applied to represent the spatial distribution of monthly precipitation. Among these, the most widely used are deterministic and geostatistical methods, including global and local models, inverse distance weighting (IDW), and kriging [28-31]. Several studies have compared different geostatistical techniques—such as splines, IDW, kriging, and cokriging—to evaluate their effectiveness [32-35]. These methods can produce a range of outputs, including kriging prediction maps, kriging standard error maps, exceedance probability maps for predefined thresholds, and quantile maps for specified probability levels. Geostatistical (kriging) models typically involve several steps: analysing groundwater variability (distribution, trends, anisotropy, and outliers), computing the empirical semivariogram or covariance, fitting a model to the empirical data, constructing the kriging system of equations, and solving it to obtain predicted groundwater values along with associated estimation errors at given locations. Among these methods, kriging has been particularly widely applied in earth sciences and hydrogeology [36-38]. Moreover, many researchers have assessed the performance of interpolation approaches such as kriging, cokriging, and kriging with external drift [5, 39]. Notably, kriging with external drift, which incorporates digital elevation model (DEM) data, has been identified as the most effective approach for mapping groundwater levels in unconfined aquifer systems [40-41].

The Empirical Bayesian Kriging (EBK) approach has been applied in various studies [42-46]. EBK is a geostatistical interpolation technique designed to overcome the challenges of constructing a valid kriging model. While traditional kriging methods require manual adjustment of model parameters, EBK automates this process through iterative simulation and subsetting [42, 47]. EBK is based on restricted maximum likelihood estimation [48-49] and accounts for uncertainty in the semivariogram model by repeatedly subsetting the data and generating multiple semivariogram realizations. This reduces the reliance on strong assumptions about semivariogram structure, making EBK particularly suitable for moderately non-stationary datasets. Moreover, EBK enhances the accuracy of prediction standard errors compared with conventional kriging approaches. A major advantage of EBK is that it eliminates the need for manual parameter calibration, as all adjustments are performed automatically during the modelling process. Unlike other kriging methods, which typically depend on user-specified semivariogram models and may struggle with small or uncertain datasets, EBK

incorporates estimation errors directly into the simulation process. As a result, it requires fewer modelling steps, provides more reliable uncertainty estimates, and achieves greater predictive accuracy, particularly when working with limited data. Finžgar et al. [50], demonstrated the effectiveness of EBK in assessing the spatial distribution of metal contamination in soils.

Building on these advantages, the present study evaluates the spatio-temporal performance of the Group Method of Data Handling (GMDH) and Empirical Bayesian Kriging in simulating groundwater elevation, with a specific focus on the Silakhor Plain in Iran.

2. Methodology

2.1 Kriging

Kriging is a geostatistical method widely employed for optimal spatial prediction in fields such as agriculture, mining, and environmental sciences. As a probabilistic predictor, it is grounded in a statistical model of spatial data. Its main advantages include the quantification of prediction uncertainty through standard errors and the minimization of prediction variance, making Kriging an unbiased and optimal estimator in the sense that the predicted values, on average, equal the true values [48]. The method relies on the semivariogram, which characterizes spatial dependence between data points as a function of their separation distance and direction.

Let Z(x) be the value of the variable Z at the point x. Given the n measurements of $Z(x_1)$,…, $Z(x_n)$ at known locations x_1,….x_n, an estimate of Z^* is achieved at a non-sampled location x_p. The Kriging estimator is given by the weighted linear combinations of the available samples.

$$Z^*(x_p) = \sum_{i=1}^{n} \lambda_i Z(x_i) \quad (1)$$

Considering the unbiasedness condition yields and γ(h) as the variogram, the kriging linear equations by which the weight can be calculated are derived in order to estimate the variance minimum by introducing Lagrange multiplier:

$$\sum_{l=1}^{v} \sum_{i=1}^{n_l} \lambda_{il} \gamma_{lv}(x_i, x_j) - \mu_v = \gamma_{uv}(x_j, x)$$
$$\sum_{i=1}^{n_l} \lambda_{il} = \begin{cases} 1, 1 = u \\ 0, 1 \neq u \end{cases} \quad (2)$$

Where $\gamma(x_i,x_j)$ is the value of variogram between location x_i and location x_j and u is covariate. All weights λ_i and Lagrange multiplier μ can be calculated; then, Z^* can be obtained by the equation (1) [51].

2.2 Empirical Bayesian Kriging

Empirical Bayesian kriging (EBK) provides an effective and simple approach to data interpolation. The EBK model differs from classical kriging models, because it accounts for the error of estimating the semi-variogram model by estimating and utilizing various semi-variogram models as opposed to one semi-variogram. Pilz et al. [43] and Finzgar et al. [50] were the first to introduce the EBK model in past research. The EBK approach is based on the principles of geostatistical interpolation while automating some of the more difficult aspects of building a valid kriging model. Other versions of the kriging methods require the analyst to manually calibrate the model parameters. The EBK will calculate these parameters automatically through a sub-setting process and simulations. The EBK process is capable of accommodating partially non-stationary input datas. The EBK approach considers the error in estimating the assumed semi-variogram model through repeated simulations [50]. Empirical Bayesian Kriging (EBK) is a refined version of traditional kriging. It improves on the classic method by allowing the estimation of multiple semivariogram models, which are then used to interpolate data based on Bayes' theorem [52].

2.3 Group Method of Data Handling

The Group Method of Data Handling (GMDH) is a family of mathematical modeling and nonlinear regression algorithms, which is originally proposed by Ivakhnenko [21]. This approach is also known as polynomial neural network and can be assumed as a specific type of supervised ANNs. In addition to modeling specifications, the GMDH model employs the concept of natural selection to regulate the size, complexity and accuracy of network. The main application of the GMDH model is modeling the complex systems, function approximation, nonlinear regression, and pattern recognition. The GMDH approach is one of the inductive approaches based on the perceptron theory that has been developed to identify systems, models and predict complex ones. The GMDH algorithm is combined with N-Adaline and is higher as compared to the structure type because the perceptron boasts the precision of classification information in the form of useful and not useful information and the number of data perceptions is less. In Figure 1, a schematic diagram of the GMDH network is shown with the structure of N-Adaline [18].

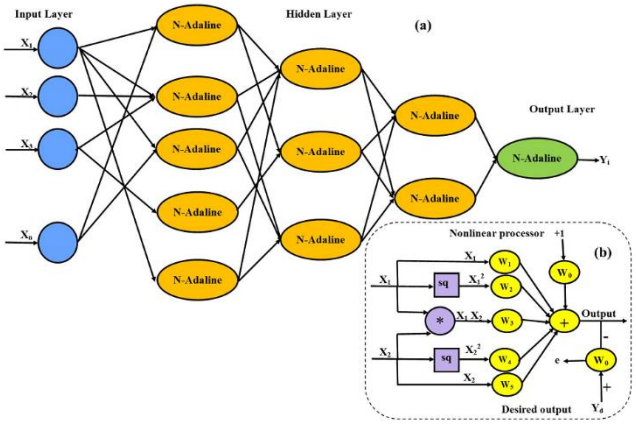

Fig.1: (a) An illustration of GMDH model, (b) N-Adaline structure

In Fig.1, Sq and * represent the square and mark, respectively and {PX_1, X_2, X_3,.., X_n} represents the model

input and Y is the output. An external benchmark to determine the network structure is defined as follows:

$$y = a_0 + \sum_{i=1}^{N} w_i x_i + \sum_{i=1}^{N}\sum_{j=1}^{N} w_{ij} x_i x_j + \sum_{i=1}^{N}\sum_{j=1}^{N}\sum_{k=1}^{N} w_{ijk} x_i x_j x_k \quad (3)$$

Where x denotes the input, y signifies the output, N indicates the count of inputs, and w refers to the weights. The regression methods are used to calculate the weighting coefficients. Consequently, the minimization must occur between the disparities of the observed and simulated results for every pair of data as input variables.

2.4 The Proposed GMDH-EBK Model

According to the capabilities of the GMDH model in temporal prediction and the EBK model in terms of spatial prediction, the hybrid model used these models in temporal-spatially prediction. The hybrid GMDH-EBK modeling process was consisted of two steps. The first step was to assemble groundwater level matrices. The monthly data sets (i.e. monthly groundwater level patterns and groundwater levels of 11 observation wells) were used to configure the GMDH model. This is a temporal prediction shown in equation (4). The second step refers to spatially forecasted groundwater levels. For this purpose, groundwater levels calculated in the previous step were used as an input into the EBK model in equation (5). Figure 2 represents the GMDH-EBK algorithm.

$$EL_{t+1} = f(P_t, EL_t, EL_{t-1}, EL_{t-2}, \dots, EL_{t-n}) \quad (4)$$

$$EL^{s}_{t+1} = f(EL^{1}_{t+1}, EL^{2}_{t+1}, EL^{3}_{t+1}, \dots, EL^{m}_{t+1}) \quad (5)$$

EL_{t+1} is the groundwater level in one month ahead using GMDH model. This variable was calculated based on groundwater levels in previous months and precipitation in the same month. Actually, GMDH model extrapolated groundwater levels for temporal prediction. After calculating the groundwater levels for each well, EBK model interpolated spatial groundwater levels. EL^{s}_{t+1} is temporal-spatial groundwater level forecasted in the hybrid model. In the equations (4) and (5), bottom and upper indices are time and location of wells, respectively.

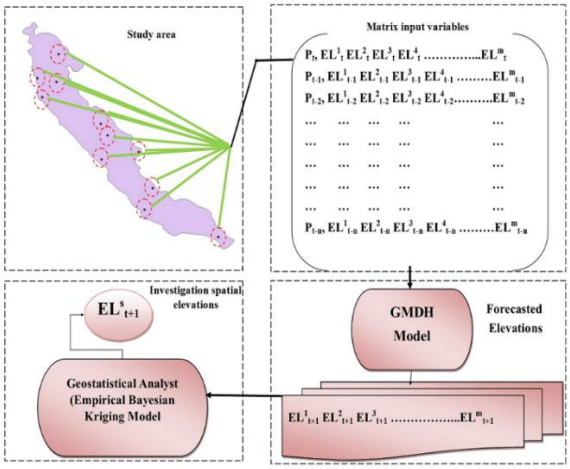

Fig. 2: Temporal- Spatial process in hybrid model

The proposed model in this study is based on the black-box hydrological model that predicts well levels according to groundwater level data associated with each other in the basin's environment.

2.5 Model Performance Criteria

The model performance was evaluated by two statistical indices: Root Mean Squared Error (RMSE), and Determination of Coefficient (DC). Equations 6 and 7 are related to these indices. The most accurate model is the one in which the values of the DC and RMSE are closer to one and zero, respectively.

$$DC = 1 - \frac{\sum_{i=1}^{n}(y_{io} - y_{ip})2}{\sum_{i=1}^{n}(y_{io} - y)2} \quad (6)$$

$$RMSE = \sqrt{\frac{\sum_{i=1}^{n}(y_{io} - y_{ip})2}{n}} \quad (7)$$

Where

y_{io}, y_{ip}, y and n are the values of observed data, simulated data, average observed data and number of data, respectively [44].

2.6 Study Area

The data utilized in this study come from the Silakhor plain, situated in the western part of Iran within Lorestan province. The Silakhor plain is an elevated region within the basin of the Karun River. Beginning at Garrin Mountain, Gelerood River flows through southern Borujerd and gathers additional streams in lower Silakhor, where it becomes known as Tireh River. The Silakhor plain lies between 33° 15' and 34° 10' Northern latitude, as well as between 48° 28' and 49° 30' Eastern longitude. The drainage basin covers an area of 2545.8 km². Silakhor is a pasture stretching from the northwest to the southeast alongside the raised terrain of the Zagros Mountains. Figure 3 shows the placement of observation wells and the study area location.

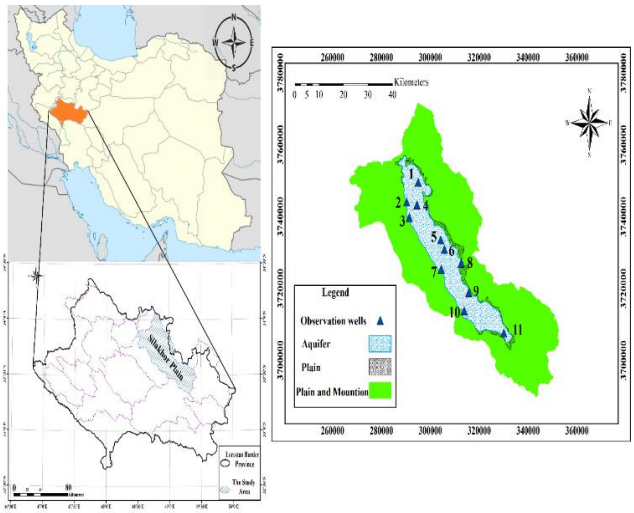

Fig. 3: Location of observation wells in study area (Silakhor plain)

The time series data for 120 months (2003–2013) were used in the modelling process (84 months for the training step and 36 months for the verification step). The statistical characteristics of groundwater levels for the Silakhor plain on monthly time scales were tabulated in Table 1. The precipitation time series were used to predict groundwater levels. The monthly precipitation time series which were used in this study and average groundwater levels are presented in Figure 4 and hydrological parameyters of study area shows in Table 2.

The Silakhor Plain was selected as the case study area owing to its semi-arid hydro-climatic conditions, marked by high variability in precipitation and temperature, which contribute to pronounced groundwater fluctuations. Over the past three decades, the plain has seen an average groundwater level decline of 2.6 meters, driven largely by over-reliance on subsurface resources amid agricultural intensification and periodic droughts. The availability of a dense piezometric monitoring network further supports detailed spatio-temporal analysis, making this basin an apt testing ground for the proposed hybrid model. Although more recent data could extend the temporal scope, this period captures substantial variability in piezometric levels, affirming the model's efficacy while setting the stage for future extensions with contemporary datasets.

Table 1. Statistic characteristics of groundwater levels data for Silakhor plain

		Calibration data set				Verification data set			
	Well Name	**Max(m)**	**Min(m)**	**Average(m)**	**Variance(m)**	**Max(m)**	**Min(m)**	**Average(m)**	**Variance(m)**
1	Chaghadon	23.06	0.0	15.82	22.17	17.64	4.93	11.57	16.91
2	Chegeni	9.49	0.72	2.51	1.49	15.56	0.54	8.25	32.02
3	Deh Haji	19.56	9.98	14.99	6.43	19.00	9.89	13.26	7.80
4	Hamyaneh	5.45	1.85	3.84	1.13	14.27	1.49	4.07	3.27
5	Kabadan	17.55	0.50	3.48	22.50	20.17	0.72	1.77	7.39
6	Sugar factory	9.63	2.52	5.24	2.76	9.63	3.46	7.44	2.23
7	Keyvareh	2.80	1.15	2.42	0.10	2.70	1.7	2.19	0.03
8	Sandrokan	8.50	4.70	6.70	0.93	7.60	3.46	6.02	0.86
9	ShokrAbad	2.65	0.85	1.58	0.20	7.31	0.93	2.05	1.17
10	Siloye Boroujerd	18.05	10.78	14.90	4.12	18.29	13.44	15.50	1.39
11	Valyan	35.17	0.0	15.46	177.24	22.58	17.36	20.09	0.97

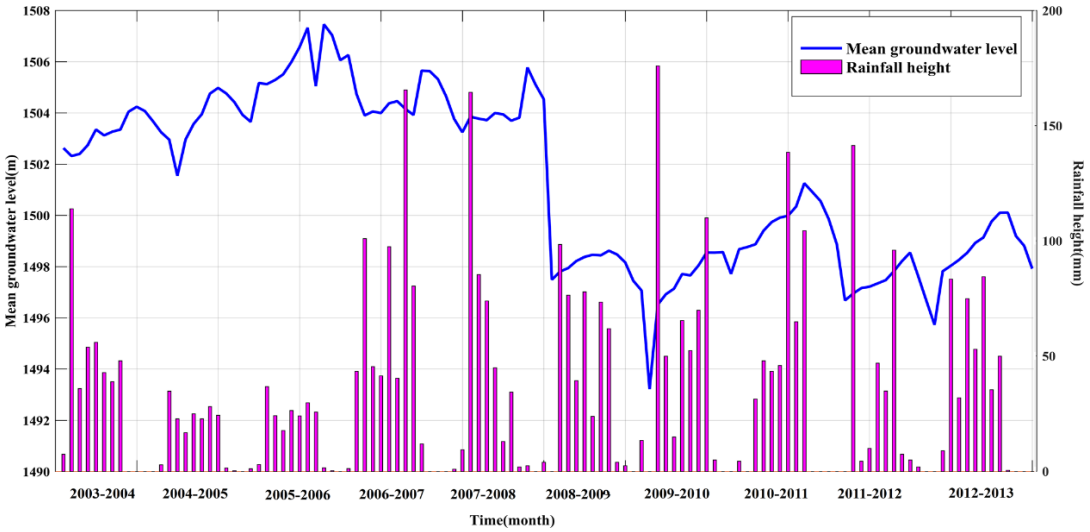

Fig. 4: Comparison of mean groundwater levels and precipitation changes in Silakhor plain

Table 2: Hydrological parameters in Silakhor plain

Monthly time series	Average	Min	Max
Rainfall(mm)	34.1	0.0	176.4
Temperature(c)	15.2	-30.0	40.4
Relative Humidity	53%	35%	63%
Evaporation(mm)	1658.7	0.0	2148.8

3. Results and Discussion

In this study, monthly observed groundwater levels from 11 observation wells in the Silakhor plain, spanning from 2003 to 2013, were utilized in the hybrid GMDH-EBK model. The dataset was divided into a training period (2003–2009) for model calibration and a verification period (2009–2013)

for performance evaluation. Details of the model inputs, configurations, and hyperparameters are provided below to ensure reproducibility. Details of the model inputs, configurations, and hyperparameters are provided below to ensure reproducibility.

For the GMDH component, which handled temporal prediction, the inputs consisted of groundwater levels from the previous three months (i.e., lags of t-1, t-2, and t-3) for each well, along with precipitation data for the previous month (t-1). No additional exogenous variables were included. The time series were standardized by subtracting the mean and dividing by the standard deviation (z-score normalization) to improve model stability, however no explicit stationarization (e.g., differencing) was applied, as the GMDH algorithm inherently adapts to non-stationary patterns through its inductive structure, leveraging the natural selection principle to optimize network complexity [21]. Feature selection was conducted automatically within the GMDH framework using a combinatorial approach, where only the most predictive quadratic polynomials were retained based on the external criterion of regularity (minimizing prediction error on a hold-out subset of the training data).

The GMDH model was implemented using a custom MATLAB script (MATLAB version R2020a), with a random seed set to 42 for reproducibility. The model was configured with a maximum of 5 layers and 10 neurones per layer to balance complexity and overfitting, as excessive layers or neurones could lead to overparameterization [18]. The stopping criterion was set to a minimum improvement in the coefficient of determination (DC) threshold of 0.001 over three consecutive iterations, ensuring efficient convergence. The fitness function used was the mean squared error (MSE), optimized to minimize forecasting errors during training. Multiple architectures were tested (e.g., varying layer/neurone limits from 3–7 and 5–15, respectively), and the optimal configuration was selected based on the lowest root mean square error (RMSE) on the verification set.

According to Equation (4), the observed data were applied as inputs to the GMDH model to forecast groundwater levels for the next month in each well. Table 3 presents the performance metrics (DC and RMSE) for the GMDH model during the verification period.

As shown in Table 3, the GMDH model yielded strong results across all wells, with the highest DC values observed for the Sandrokan and Hamyaneh wells (both 0.95), indicating excellent predictive accuracy. The maximum RMSE was 0.32 m for the Shokrabad well, reflecting relatively higher variability in that location. Figure 5 illustrates the comparison between observed and computed groundwater levels for selected wells (Chaghadon, Hamyaneh, Sugar factory, and Valyan) during the verification period. The GMDH network was constructed iteratively, with polynomial coefficients derived via ordinary least squares on the training data. The model's advantages, including optimal complexity selection and minimal forecasting error variance, make it particularly suitable for small datasets like this one that align with inductive modelling principles in computational intelligence.

Table 3: Performance parameters for GMDH model in forecasting groundwater level in the verification period

	Well Name	Xutm	Yutm	DC	RMSE(m)
1	Chaghadon	329691	3707154	0.91	0.22
2	Chegeni	291019	3739282	0.72	0.24
3	Deh Haji	305354	3730453	0.75	0.27
4	Hamyaneh	313505	3713414	0.95	0.18
5	Kabadan	294646	3749151	0.75	0.24
6	Sugar factory	315364	3718390	0.85	0.18
7	Keyvareh	304103	3744958	0.74	0.21
8	Sandrokan	294160	3742822	0.95	0.26
9	ShokrAbad	289962	3743665	0.89	0.32
10	Siloye Broujerd	303874	3733139	0.71	0.25
11	Valyan	312279	3726654	0.79	0.22

In the subsequent step, spatial prediction was performed using geostatistical analysis in ArcGIS (version 10.8). The temporally forecasted groundwater levels from the GMDH model served as inputs to the EBK model. EBK's key strength lies in its ability to account for semivariogram estimation uncertainty by simulating multiple semivariograms (100 in this case) and weighting them via Bayes' rule [48-49]. This results in zero estimation variance at sampling points, ensuring that the interpolated surface honours the input data precisely.

For the detrended EBK variants, a linear trend removal was applied, assuming a first-order polynomial surface to account for regional gradients (e.g., northeastward deepening of groundwater levels due to terrain influences). No digital elevation model (DEM)-based drift was incorporated, as the focus was on data-driven detrending. The final variogram parameters for the best-performing EBK model (K-Bessel Detrended) were nugget = 0.05 m², partial sill = 0.15 m², total sill = 0.20 m², and range = 15 km. Uncertainty estimates, derived from the standard error of prediction across 100 simulations, averaged 0.18 m, with a 95% confidence interval width of approximately 0.35 m at unsampled locations.

Table 4 summarizes the performance parameters (DC and RMSE) for the hybrid model, comparing EBK variants against other kriging methods (ordinary, simple, and disjunctive) during the verification period.

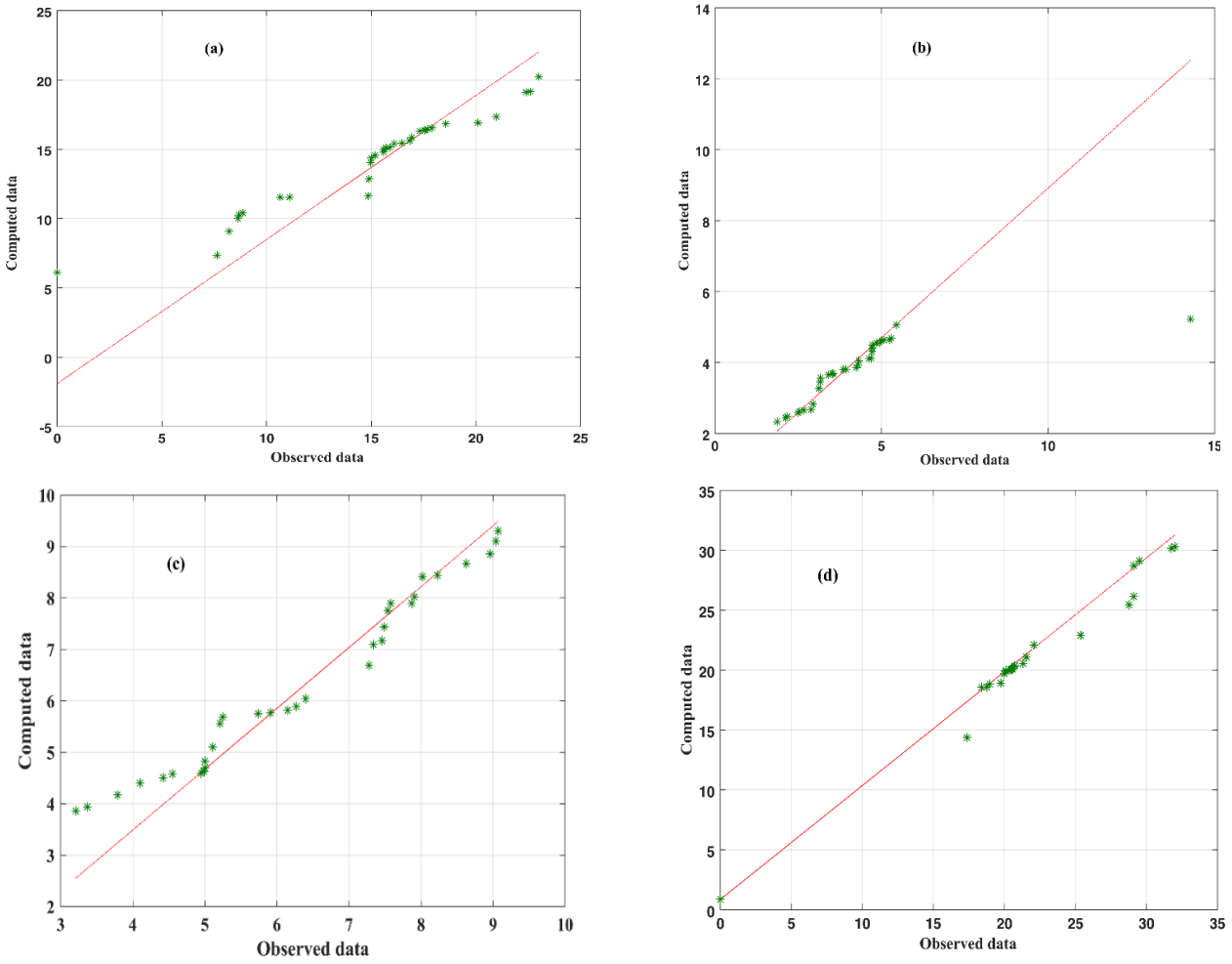

Fig. 5: Comparison of observed data and computed data for (a) Chaghadon, (b) Hamyaneh, (c) Sugar factory, (d) Valyan wells in verification period (m)

Table 4: Performance parameters in Hybrid model in forecasting groundwater levels in comparison with kriging models

Interpolation method	Variogram	DC	RMSE(m)
EBK	K-Bessel Detrended	0.83	0.20
	K-Bessel	0.81	0.21
	Whittle Detrended	0.81	0.21
	Exponential Detrended	0.8	0.22
Ordinary	Circular	0.45	0.23
	Spherical	0.78	0.23
	Gaussian	0.68	0.22
	Exponential	0.75	0.24
Simply	Circular	0.69	0.23
	Spherical	0.77	0.23
	Gaussian	0.42	0.22
	Exponential	0.51	0.25
Disjonctive	Circular	0.76	0.23
	Spherical	0.77	0.23
	Gaussian	0.78	0.22
	Exponential	0.75	0.25

As indicated in Table 4, the EBK model with the K-Bessel Detrended variogram achieved the best performance, with a DC of 0.83 and RMSE of 0.20 m, outperforming other EBK variants and all ordinary, simple, and disjunctive kriging models. The confusion in the original manuscript regarding the simple exponential model has been clarified: the K-Bessel Detrended model consistently showed the highest DC (0.83) and lowest RMSE (0.20 m). The lowest DC values were observed for the ordinary circular (0.45) and simple Gaussian (0.42) models. EBK's superior results stem from its handling of semivariogram uncertainty through repeated simulations and Bayesian weighting, unlike deterministic methods such as inverse distance weighting (IDW), which lack built-in error estimation for variograms. The semivariogram was computed as half the average squared difference between paired measurements at lag distances (h), providing a robust measure of spatial continuity.

Figure 6 presents the semivariograms derived from the EBK model within the GMDH-EBK hybrid framework, illustrating the spatial autocorrelation of groundwater levels across various lag distances. The subplots (a) to (d) show

different variogram models. The blue crosses represents the observed data points, and the red lines represents the fitted models, along with confidence intervals (purple dashed lines). The K-Bessel Detrended variogram (subplot a) demonstrates the highest correlation and best fit, achieving a coefficient of determination (DC) of 0.83 and an RMSE of 0.20 m, confirming its superior performance in interpolating temporal-spatial groundwater levels. This method enables precise estimation of water height variations, facilitating targeted strategies for managing groundwater depletion or recharge. Analysis of population centers and well extraction trends around the study area further reveals a northeastward decline in groundwater levels, consistent with regional hydrogeological patterns and human activity impacts.

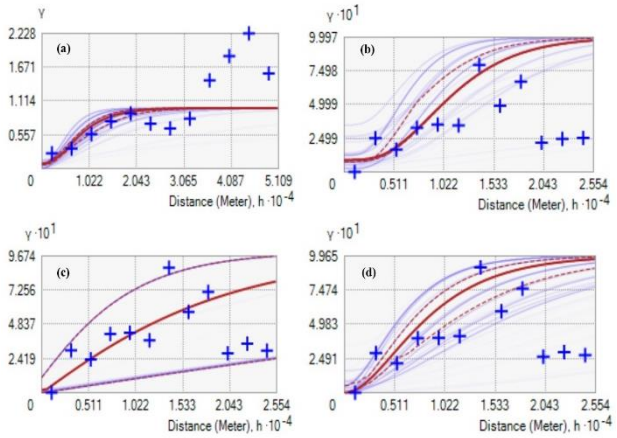

Fig. 6: Variogram models for groundwater level, (a) K-Bessel, (b) K-Bessel Detrended, (c) Exponential Detrended, (d) Whittle Detrended

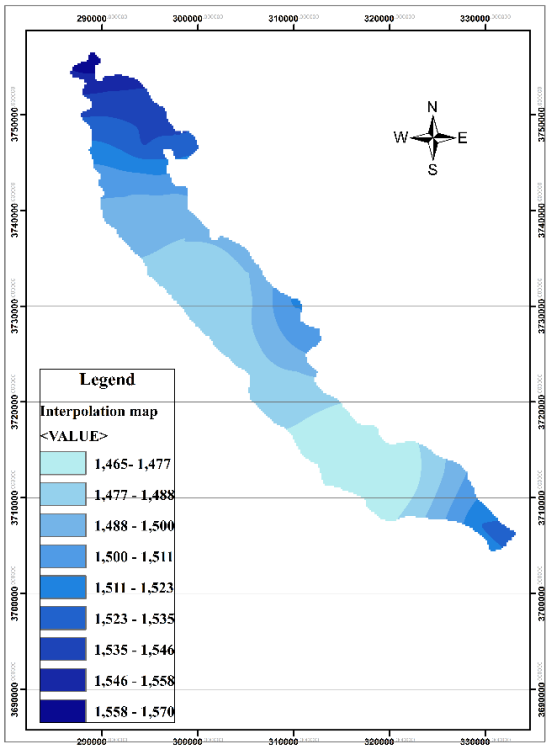

Fig. 7: The change of groundwater level contour line using hybrid model (m)

Figure 7 depicts the groundwater level contour lines generated by the hybrid model, revealing a northeastward trend in level fluctuations, consistent with topographic influences and population-driven extraction around wells. This visualization aids in identifying potential drilling sites and imputing missing data.

4. Limitations and Future Work

While this study demonstrates the effectiveness of the proposed hybrid model for spatio-temporal prediction of groundwater levels in the Silakhor Plain, certain limitations should be acknowledged. First, the model was evaluated using a single train/test split (2003–2009 for training and 2009–2013 for testing), which may not fully capture its stability across different temporal regimes. For instance, hydro-climatic conditions, such as precipitation patterns or drought events, vary over time, and a single split may reflect performance specific to the chosen period. Additionally, the model was trained and tested on data from all monitoring wells in the study area, potentially benefiting from spatial autocorrelation among closely located wells. This design does not test the model's ability to generalize to unseen locations, limiting insights into its spatial transferability.

To address these limitations, future work will focus on enhancing the model's generalizability. A rolling window cross-validation approach will be implemented, partitioning the time series into multiple consecutive folds (e.g., training on 2003–2007 and testing on 2007–2009, then training on 2003–2008 and testing on 2008–2010). This will allow us to assess the model's performance across diverse temporal conditions, ensuring robustness against seasonal or climatic variability. Furthermore, a leave-one-location-out (LOLO) cross-validation strategy will be employed, where one well is iteratively held out, and the model is trained on the remaining wells to predict the held-out well's groundwater levels. This approach will evaluate the model's ability to generalize to new locations, a critical requirement for broader applicability in groundwater management. Additionally, incorporating more recent data (post-2013) from regional water authorities will strengthen the model's relevance to current conditions. These enhancements will provide a more comprehensive understanding of the model's capabilities and support its application in other hydrogeological settings.

5. Conclusions

In conclusion, the global water challenge, driven by rising population growth and diminishing water resources, poses significant concerns, particularly for developing nations like Iran, necessitating effective management strategies and comprehensive plans. This study introduces a novel hybrid approach by combining the GMDH and EBK models to predict temporal-spatial groundwater levels, leveraging the

strengths of artificial intelligence techniques that have gained prominence for their accuracy in water resource modelling. Utilizing a decade of data from the Silakhor plain, the model achieved high predictive accuracy, with notable determination coefficients of 0.95 for Hamyaneh, 0.91 for Chaghadon, 0.85 for the Sugar Factory, and 0.79 for Valyan, demonstrating its reliability. The method's ability to estimate unmeasured water levels and its adaptability for future applications, considering varying depths, underscore its potential as a valuable tool for sustainable groundwater management in the region.

References

[1] Nourani, V., Monadjemi, P. and Singh, V.P., 2007. Liquid analog model for laboratory simulation of rainfall–runoff process. *Journal of Hydrologic Engineering*, *12*(3), pp.246-255.

[2] Nazir, H.M., Hussain, I., Faisal, M., Shoukry, A.M., Gani, S. and Ahmad, I., 2019. Development of Multidecomposition Hybrid Model for Hydrological Time Series Analysis. *Complexity*, *2019*.

[3] Zhao, Q., Zhu, Y., Wan, D., Yu, Y. and Cheng, X., 2018. Research on the Data-Driven Quality Control Method of Hydrological Time Series Data. *Water*, *10*(12), p.1712.

[4] Komasi, M., Sharghi, S. and Safavi, H.R., 2018. Wavelet and cuckoo search-support vector machine conjugation for drought forecasting using standardized precipitation index (case study: Urmia Lake, Iran). *Journal of Hydroinformatics*, p.jh2018115.

[5] Bhat, S., Motz, L.H., Pathak, C. and Kuebler, L., 2012. Designing a Groundwater-Level Monitoring Network Using Geostatistics: A Case Study for South and Central Florida, USA. In *World Environmental and Water Resources Congress 2012: Crossing Boundaries* (pp. 48-58).

[6] Singh, A., Panda, S.N., Uzokwe, V.N. and Krause, P., 2019. An assessment of groundwater recharge estimation techniques for sustainable resource management. *Groundwater for Sustainable Development*, *9*, p.100218.

[7] Darras, T., Estupina, V.B., Kong-A-Siou, L., Vayssade, B., Johannet, A. and Pistre, S., 2015. Identification of spatial and temporal contributions of rainfalls to flash floods using neural network modelling: case study on the Lez basin (southern France). *Hydrology and Earth System Sciences*, *19*(10), p.4397.

[8] Demirel, M.C., Booij, M. and Hoekstra, A., 2015. The skill of seasonal ensemble low-flow forecasts in the Moselle River for three different hydrological models. *Hydrology and earth system sciences*.

[9] Chang, F.J., Chang, L.C., Huang, C.W. and Kao, I.F., 2016. Prediction of monthly regional groundwater levels through hybrid soft-computing techniques. *Journal of hydrology*, *541*, pp.965-976.

[10] Alizadeh, M.J., Nourani, V., Mousavimehr, M. and Kavianpour, M.R., 2017. Wavelet-IANN model for predicting flow discharge up to several days and months ahead. *Journal of Hydroinformatics*, p.jh2017142.

[11] Abiye, T., Masindi, K., Mengistu, H. and Demlie, M., 2018. Understanding the groundwater-level fluctuations for better management of groundwater resource: A case in the Johannesburg region. *Groundwater for Sustainable Development*, *7*, pp.1-7.

[12] Wagh, V., Panaskar, D., Muley, A., Mukate, S. and Gaikwad, S., 2018. Neural network modelling for nitrate concentration in groundwater of Kadava River basin, Nashik, Maharashtra, India. *Groundwater for Sustainable Development*, *7*, pp.436-445.

[13] Wunsch, A., Liesch, T. and Broda, S., 2020. Groundwater level forecasting with artificial neural networks: A comparison of LSTM, CNN and NARX. Hydrology and Earth System Sciences Discussions, 2020, pp.1-23.

[14] Fabio, D.N., Abba, S.I., Pham, B.Q., Towfiqul Islam, A.R.M., Talukdar, S. and Francesco, G., 2022. Groundwater level forecasting in Northern Bangladesh using nonlinear autoregressive exogenous (NARX) and extreme learning machine (ELM) neural networks. Arabian Journal of Geosciences, 15(7), p.647.

[15] Hoque, M.A., Apon, A.A., Hassan, M.A., Adhikary, S.K. and Islam, M.A., 2024. Enhanced Forecasting of Groundwater Level Incorporating an Exogenous Variable: Evaluating Conventional Multivariate Time Series and Artificial Neural Network Models. Geographies, 5(1), p.1.

[16] Kishor, K., Aggarwal, A., Srivastava, P.K., Sharma, Y.K., Lee, J. and Ghobadi, F., 2025. A Systematic Literature Review of MODFLOW Combined with Artificial Neural Networks (ANNs) for Groundwater Flow Modelling. Water, 17(16), p.2375.

[17] Isık, H. and Akkan, T., 2025. Water quality assessment with artificial neural network models: Performance comparison between SMN, MLP and PS-ANN methodologies. Arabian Journal for Science and Engineering, 50(1), pp.369-387.

[18] Barzegar, R., Fijani, E., Moghaddam, A.A. and Tziritis, E., 2017. Forecasting of groundwater level fluctuations using ensemble hybrid multi-wavelet neural network-based models. *Science of the Total Environment*, *599*, pp.20-31.

[19] Shabri, A. and Samsudin, R., 2014. A Hybrid GMDH and Box-Jenkins Models in Time Series Forecasting. *Applied Mathematical Sciences*, *8*(62), pp.3051-3062.

[20] De Giorgi, M.G., Malvoni, M. and Congedo, P.M., 2016. Comparison of strategies for multi-step ahead photovoltaic power forecasting models based on hybrid group method of data handling networks and least square support vector machine. *Energy*, *107*, pp.360-373.

[21] Ivakhnenko, A.G. 1968. The Group Method of Data Handling-a Rival of the Method of Stochastic Approximation, Soviet Automatic Control c/c of Avtomatika, 1: 43-55.

[22] Lambert, R.S., Lemke, F., Kucherenko, S.S., Song, S. and Shah, N., 2016. Global sensitivity analysis using sparse high dimensional model representations generated by the group method of data handling. *Mathematics and Computers in Simulation*, *128*, pp.42-54.

[23] Amiri-Doumari, S., Karimipour, A., Nayebpour, S.N. and Hatamiafkoueieh, J., 2022. Integration of group method of data handling (GMDH) algorithm and population-based metaheuristic algorithms for spatial prediction of potential groundwater. Environmental Earth Sciences, 81(20), p.485

[24] Amini, H., Ashrafzadeh, A. and Khaledian, M., 2024. Enhancing groundwater salinity estimation through integrated GMDH and geostatistical techniques to minimize Kriging interpolation error. Earth Science Informatics, 17(1), pp.283-297.

[25] Lal, A., Sharan, A., Sharma, K., Ram, A., Roy, D.K. and Datta, B., 2024. Scrutinizing different predictive modeling validation methodologies and data-partitioning strategies: new insights using groundwater modeling case study. Environmental Monitoring and Assessment, 196(7), p.623.

[26] Murmu, P., Kumar, M., Lal, D., Sonker, I. and Singh, S.K., 2019. Delineation of groundwater potential zones using geospatial techniques and analytical hierarchy process in Dumka district, Jharkhand, India. *Groundwater for Sustainable Development*, p.100239.
[27] Dummer, T.J.B., Yu, Z.M., Nauta, L., Murimboh, J.D. and Parker, L., 2015. Geostatistical modelling of arsenic in drinking water wells and related toenail arsenic concentrations across Nova Scotia, Canada. *Science of the Total Environment*, *505*, pp.1248-1258.
[28] Feizizadeh, B., Roodposhti, M.S., Jankowski, P. and Blaschke, T., 2014. A GIS-based extended fuzzy multi-criteria evaluation for landslide susceptibility mapping. *Computers & geosciences*, *73*, pp.208-221.
[29] Elbeih, S.F., 2015. An overview of integrated remote sensing and GIS for groundwater mapping in Egypt. *Ain Shams Engineering Journal*, *6*(1), pp.1-15.
[30] Huang, J., Huang, Y., Pontius, R.G. and Zhang, Z., 2015. Geographically weighted regression to measure spatial variations in correlations between water pollution versus land use in a coastal watershed. Ocean & Coastal Management, 103, pp.14-24.
[31] Javari, M., 2015. A study of impacts of temperature components on precipitation in Iran using SEM-PLS-GIS. *Journal of Earth Science & Climatic Change*, (S3), p.1.
[32] Karacan, C.Ö., Olea, R.A. and Goodman, G., 2012. Geostatistical modeling of the gas emission zone and its in-place gas content for Pittsburgh-seam mines using sequential Gaussian simulation. *International journal of coal geology*, *90*, pp.50-71.
[33] Karagiannis-Voules, D.A., Odermatt, P., Biedermann, P., Khieu, V., Schär, F., Muth, S., Utzinger, J. and Vounatsou, P., 2015. Geostatistical modelling of soil-transmitted helminth infection in Cambodia: Do socioeconomic factors improve predictions?. *Acta tropica*, *141*, pp.204-212.
[34] Mentis, D., Hermann, S., Howells, M., Welsch, M. and Siyal, S.H., 2015. Assessing the technical wind energy potential in Africa a GIS-based approach. *Renewable Energy*, *83*, pp.110-125
[35] Belkhiri, L., Mouni, L., Narany, T.S. and Tiri, A., 2017. Evaluation of potential health risk of heavy metals in groundwater using the integration of indicator kriging and multivariate statistical methods. *Groundwater for Sustainable Development*, *4*, pp.12-22.
[36] Plain, G., 2012. A geo-statistical approach to the change procedure study of under-ground water table in a GIS framework, case study: Razan-Ghahavand Plain, Hamedan Province, Iran. *Journal of Academic and Applied Studies*, *2*(11), pp.56-69.
[37] Canoğlu, M.C. and KURTULUŞ, B., 2017. Determination of the dam axis permeability for the design and the optimization of grout curtain: An example from Orhanlar Dam (Kütahya-Pazarlar). *Periodicals of Engineering and Natural Sciences (PEN)*, *5*(1).
[38] Varouchakis, E.A., 2018. Spatiotemporal geostatistical modelling of groundwater level variations at basin scale: a case study at Crete's Mires Basin. *Hydrology Research*, *49*(4), pp.1131-1142.
[39] Pardo-Igúzquiza, E. and Chica-Olmo, M., 2007. KRIGRADI: A cokriging program for estimating the gradient of spatial variables from sparse data. *Computers & Geosciences*, *33*(4), pp.497-512.
[40] Desbarats, A.J., Logan, C.E., Hinton, M.J. and Sharpe, D.R., 2002. On the kriging of water table elevations using collateral information from a digital elevation model. Journal of Hydrology, 255(1-4), pp.25-38.
[41] Rivest, M., Marcotte, D. and Pasquier, P., 2008. Hydraulic head field estimation using kriging with an external drift: A way to consider conceptual model information. *Journal of hydrology*, *361*(3-4), pp.349-361.
[42] Szentimrey, T., Bihari, Z. and Szalai, S., 2007. Comparison of geostatistical and meteorological interpolation methods (what is what?). *Spatial interpolation for climate data: the use of GIS in climatology and meteorology*, pp.45-56.
[43] Pilz, J., Kazianka, H. and Spöck, G., 2012. Some advances in Bayesian spatial prediction and sampling design. *Spatial Statistics*, *1*, pp.65-81.
[44] Komasi, M. and Goudarzi, H., 2019. The Application of the Entropy and Empirical Basin Kriging for the Optimization and Spatial Interpolation of Groundwater Monitoring Network (Case Study: Silakhor Plain). Journal of Hydrogeomorphology, 6(19), pp.145-162.
[45] Li, Y., Hernandez, J.H., Aviles, M., Knappett, P.S., Giardino, J.R., Miranda, R., Puy, M.J., Padilla, F. and Morales, J., 2020. Empirical Bayesian Kriging method to evaluate inter-annual water-table evolution in the Cuenca Alta del Río Laja aquifer, Guanajuato, México. Journal of Hydrology, 582, p.124517.
[46] Zaresefat, M., Derakhshani, R. and Griffioen, J., 2024. Empirical Bayesian Kriging, a robust method for spatial data interpolation of a large groundwater quality dataset from the Western Netherlands. Water, 16(18), p.2581.
[47] Pilz, J. and Spöck, G., 2008. Why do we need and how should we implement Bayesian kriging methods. *Stochastic Environmental Research and Risk Assessment*, *22*(5), pp.621-632.
[48] Krivoruchko, K., 2012. Empirical bayesian kriging. *ArcUser Fall*, pp.6-10.
[49] Bhunia, G.S., Shit, P.K. and Maiti, R., 2018. Comparison of GIS-based interpolation methods for spatial distribution of soil organic carbon (SOC). *Journal of the Saudi Society of Agricultural Sciences*, *17*(2), pp.114-126.
[50] Finzgar, N., Jez, E., Voglar, D. and Lestan, D., 2014. Spatial distribution of metal contamination before and after remediation in the Meza Valley, Slovenia. *Geoderma*, *217*, pp.135-143.
[51] Huang, Z., Wang, H. and Zhang, R., 2012. An improved kriging interpolation technique based on SVM and its recovery experiment in oceanic missing data. *American Journal of Computational Mathematics*, *2*(01), p.56.
[52] Seyedmohammadi, J., Esmaeelnejad, L. and Shabanpour, M., 2016. Spatial variation modelling of groundwater electrical conductivity using geostatistics and GIS. *Modeling earth systems and environment*, *2*(4), pp.1-10.